Cancer Research

Oncogenic HRAS Activates Epithelial-to-Mesenchymal Transition and Confers Stemness to *p53*-Deficient Urothelial Cells to Drive Muscle Invasion of Basal Subtype Carcinomas

Feng He[1,2], Jonathan Melamed[3], Moon-shong Tang[4], Chuanshu Huang[4], and Xue-Ru Wu[1,2,3]

Abstract

Muscle-invasive urothelial carcinomas of the bladder (MIUCB) exhibit frequent receptor tyrosine kinase alterations, but the precise nature of their contributions to tumor pathophysiology is unclear. Using mutant HRAS (HRAS*) as an oncogenic prototype, we obtained evidence in transgenic mice that RTK/RAS pathway activation in urothelial cells causes hyperplasia that neither progresses to frank carcinoma nor regresses to normal urothelium through a period of one year. This persistent hyperplastic state appeared to result from an equilibrium between promitogenic factors and compensatory tumor barriers in the p19–MDM2–p53–p21 axis and a prolonged G_2 arrest. Conditional inactivation of p53 in urothelial cells of transgenic mice expressing HRAS* resulted in carcinoma *in situ* and basal-subtype MIUCB with focal squamous differentiation resembling the human counterpart. The transcriptome of microdissected MIUCB was enriched in genes that drive epithelial-to-mesenchymal transition, the upregulation of which is associated with urothelial cells expressing multiple progenitor/stem cell markers. Taken together, our results provide evidence for RTK/RAS pathway activation and p53 deficiency as a combinatorial theranostic biomarker that may inform the progression and treatment of urothelial carcinoma. *Cancer Res; 75(10); 2017–28. ©2015 AACR.*

Introduction

Muscle-invasive urothelial carcinoma of the bladder (MIUCB) is amongst the most aggressive and deadliest cancers (1). Because of its high risk of progression to metastatic stages, MIUCB often calls for multiagent neoadjuvant chemotherapy followed by radical cystectomy or adjuvant chemotherapy after the surgery or radiotherapy concomitant with systemic chemotherapy (2, 3). Despite such debilitating therapies, over 50% of MIUCB advance to local and distant metastasis, at which point the 5-year survival rates are only about 30% and 5%, respectively (1).

A significant recent development is the recognition that MIUCB is not a single disease entity but comprises distinct subtypes distinguishable by combinatorial molecular signatures and divergent clinical outcomes (4–11). While the exact number, interrelationship, and spectra of the molecular signatures between different subtypes from different studies remain to be delineated, a consensus is emerging pointing to at least two major subtypes: luminal and basal. The luminal subtype bears features of the luminal umbrella cells of normal urothelium, for example, high levels of uroplakins, cytokeratin 20, and E-cadherin (4–6, 9–11). Mutations of fibroblast growth factor 3 (FGFR3) and tuberous sclerosis 1 (TSC1) are prevalent along with alterations involving many other genes. The basal subtype, on the other hand, expresses abundant proteins associated with the basal cells of normal urothelium, such as cytokeratins 14, 5, and 6B as well as markers signifying increased stemness and epithelial-to-mesenchymal transition (EMT; e.g., high CD44, TWIST1/2, SNAI2, ZEB2, VIM, and N-cadherin and low E-cadherin and claudin; refs. 4–6, 9, 10). Focal squamous differentiation is common in this subtype and, as suspected, the basal subtype is much more aggressive and correlates with more advanced stage and poorer prognosis than is the luminal subtype (4, 8, 10). Notably, the frequency of p53 mutations that characterize MIUCB in general does not differ significantly between the two major subtypes, although one study found RB1 pathway alterations to be more prevalent in the basal subtype than in the luminal subtype (5).

Notwithstanding the recent progress in subtyping MIUCB, several critical issues remain. First and foremost, are different subtypes of MIUCB caused by distinct genetic drivers? Thus far, most subclassification studies are based on expression signatures including those of uroplakins, cytokeratins, and cadherins (9–11), which are not genetic tumor drivers but phenotypic consequences of urothelial differentiation vis-à-vis

[1]Department of Urology, New York University School of Medicine, New York, New York. [2]Veterans Affairs New York Harbor Healthcare System, Manhattan Campus, New York, New York. [3]Department of Pathology, New York University School of Medicine, New York, New York. [4]Department of Environmental Medicine, New York University School of Medicine, New York, New York.

Note: Supplementary data for this article are available at Cancer Research Online (http://cancerres.aacrjournals.org/).

Corresponding Author: Xue-Ru Wu, Department of Urology, New York University School of Medicine, Veterans Affairs Medical Center in Manhattan, 423 E23 Street, 18th Floor, Room 18064 South, New York, NY 10010. Phone: 212-951-5429; Fax: 212-951-5424; E-mail: xue-ru.wu@med.nyu.edu

doi: 10.1158/0008-5472.CAN-14-3067

dedifferentiation. Those making use of gene mutations for subclassification often involve multiple alterations (8) whose relationship with a particular subtype remains correlative. A definitive cause–consequence effect between a minimum essential set of genetic drivers and a given subtype requires experimental verification using biologically relevant systems. Such biologic studies are important because defining the genetic driver(s) could not only simplify the subtyping of MIUCB and reduce the number of prognosticators, but also narrow down druggable targets for precise therapeutic intervention (12). Second, do different subtypes of MIUCB progress via divergent phenotypic pathways? Clinicopathological studies have long held that MIUCB can (i) arise *de novo* (i.e., without a defined precursor), (ii) progress from flat, carcinoma in situ (CIS) precursor lesions, or (iii) progress from high-grade, noninvasive papillary urothelial carcinomas (13–16). It is crucially important to determine whether some of the MIUCB subtypes are actually a result of tumor progression from a particular premalignant lesion, so that specific strategies can be devised to predict and prevent progression. Third, do different MIUCB subtypes originate from different normal urothelial cell types? Normal urothelium can be divided into at least three different compartments: basal, intermediate, and luminal (17). Although all urothelial carcinomas were previously thought to derive from the normal urothelial stem cells residing in the basal zone, recent studies suggest otherwise (16, 18). In particular, chemical carcinogenesis using a bladder-specific carcinogen, N-butyl-N-(4-hydroxybutyl)nitrosamine (BBN), coupled with lineage tracing, suggests that low-grade noninvasive and high-grade MIUCB originate from intermediate and basal compartments, respectively (19, 20). It remains an open question, however, as to whether the different subtypes within MIUCB can also originate from different normal urothelial subtypes. Finally, are different MIUCB subtypes molecularly and phenotypically static or are they quite dynamic and interchangeable reflecting different stages of dedifferentiation and tumor progression? In other words, could the luminal subtype dedifferentiate and transition into the basal subtype during the course of tumor progression? Conversely, could the basal subtype regain the ability to differentiate into the luminal subtype thus becoming less aggressive subsequent to radio- and/or chemotherapy?

To begin to tackle some of these questions, we took an in-depth look of the effects of HRAS activation and p53 deficiency using a blend of *in vitro* and *in vivo* approaches. Activation of the RTK/RAS pathway and inactivation of the p53 pathway, events that were previously thought to define low-grade noninvasive and high-grade MIUCB, respectively (13, 21, 22), were recently found in whole-genome analyses to be equally prevalent in high-grade MIUCB (72% with RTK/RAS activation and 76% with p53 pathway activation; ref. 23). This suggests that alterations affecting both signaling pathways could overlap, simply by chance, in at least 50% of the MIUCB. One scenario is that this overlap is merely due to genetic drifting of two common events that do not necessarily cross-talk and are of no consequence to tumorigenesis. Another scenario is that these two events functionally converge as a result of selective pressure in tumor cells and that they collaborate or even synergize to exert a tumor-driving role leading to the formation of MIUCB. In this study, we examine these two competing hypotheses and our results have important implications on the molecular pathogenesis of MIUCB and shed light on how some of the MIUCB subtypes can be better managed clinically.

Materials and Methods

Transgenic, knockout, and compound mice

The transgenic mouse line, *Upk2*-HRAS*, harbored a single-copy transgene comprising a 3.6-kB murine uroplakin II promoter (UPII) and a constitutively active HRAS gene (24). The urothelial expression level of the HRAS* in this low-copy *Upk2*-HRAS* line is equivalent to that of the endogenous wild-type *Ras*, as evidenced by real-time PCR and Western blotting (24). The second transgenic line, *Upk2*-cre harbored a transgene comprising the UPII and a 1.4-kB cre recombinase gene (25). The third transgenic line harbored a "floxed" *p53* allele (e.g., $p53^{LOX}$) where loxP sites were inserted in introns 4 and 6, allowing deletion of exons 5 and 6 upon cre expression (26). The identity of *Upk2*-HRAS* and *Upk2*-cre was verified by Southern blotting and that of $p53^{LOX}$ by genomic PCR. Intercrosses were carried out among these three lines with additional crosses among their offspring, yielding a number of genotypes, from which four major genotypes were chosen for phenotypic characterization: (i) *Upk2*-cre (as negative control), (ii) *Upk2*-$HRAS^{*/WT}$, (iii) *Upk2*-cre/$p53^{LOX/LOX}$, and (iv) *Upk2*-$HRAS^{*/WT}$/*Upk2*-cre/$p53^{LOX/LOX}$. All animal experiments were approved by Institutional Animal Care and Use Committee.

Laser-capture microdissection and expression arrays

Since urinary bladders of *Upk2*-cre mice exhibited normal urothelia and those of *Upk2*-$HRAS^{*/WT}$/*Upk2*-cre/$p53^{LOX/LOX}$ compound mice exhibited CIS and muscle-invasive lesions, these bladders were used for cross-sectioning and laser-capture microdissection. Briefly, 30 μm thick frozen sections were lightly stained with hematoxylin and the aforementioned lesions were dissected out using Leica LMD6000 Laser Micro-Dissection System. Total RNAs were extracted using RNeasy Micro Kit (Qiagen) and the RNA quality was verified by high-performance liquid chromatography. Microarray was carried out with Affymetrix 3′ IVT mouse expression arrays at our in-house facility (GEO accession number: GSE64756). Primary data were analyzed at the Center for Applied Genomics in University of Medicine and Dentistry of New Jersey and pathway and bioprocess analyses were performed online using Ingenuity iReport.

Cell culture, transfection, and establishment of stable lines

Human bladder urothelial carcinoma cell line, RT4, originally isolated from a low-grade, noninvasive urothelial carcinoma (27), was purchased from ATCC, maintained in McCoy's 5A medium containing 10% FBS and used within 6 months of receipt. Authentication of RT4 at ATCC used short tandem repeat profile and isoenzyme analysis. An shRNA of mouse *p53* (5′-gactccagtggtaatctact-3′) was subcloned into retroviral vector, pMKO.1-puro (Addgene) and the resultant pMKO.1-puro/sh-p53 was cotransfected with pCL-10A1 packaging vector (Novus Biologicals) into cultured Phoenix cells. The packaged virus in the supernatant was collected and used to infect RT4 cells. Following a 10-day selection in culture medium containing 1 μg/mL puromycin, survived single clones were verified for p53 knockdown. $HRAS^{WT}$ and $HRAS^{V12}$ were subcloned separately into retroviral

vector, pBABE-hygro (Addgene), and cotransfected with the pCL-10A1 packaging vector into the Phoenix cells. The packaged retroviruses were isolated and infected into RT4 cells stably expressing the shRNA-p53. Stable clones were selected in culture medium containing 200 μg/mL hygromycin for 10 days and the resultant stable clones were verified for desired gene expression.

Cell migration and invasion assays

Cell migration of stable cell lines was first compared by wound-healing assay. When cultured cells reached 80% confluence, wounds were introduced under an inverted microscope using a sterile pipette tip. Wounded cells were cultured in fresh medium for 3 days before phase-contrast images were recorded. For invasion assay, BioCoat Matrigel Invasion Chamber (BD Biosciences) was used. Briefly, stable clones (2.5×10^4 cells) were seeded in 24-well chambers (in triplicate) containing 20 ng/mL 12-O-tetradecanoylphorbol-13-acetate. After incubation for 72 hours, the noninvading cells atop the membrane were removed by scrapping and, the invading cells underneath the membrane were visualized using Diff-Quik stain and counted in five high-power (×200) microscopic fields (one-center and four-peripheral).

Cell proliferation assay

Stably transfected cells (2×10^3/well) were cultured for 48 hours and quantified by 3-(4,5-dimethylthiazol-2-yl)-2,5-diphenyltetrazoliumbromide) method (Bio-Rad).

Cell-cycle analysis

Urinary bladders were inverted to expose the mucosa. After incubation in a solution containing 1 mg/mL dispase at 4°C overnight, the urothelial cells were gently scraped off and digested with a solution containing 0.25% trypsin-EDTA at 37°C for 30 minutes. The cells were washed in PBS by centrifugation at 800 g for 5 minutes and filtered through a 100-μm pore size filter, fixed with precooled 70% ethanol at 4°C, and stained with 40 μg/mL propidium iodide containing 100 μg/mL RNase. Cell sorting was carried out using Facscan (Beckman) and the data were analyzed using ModiFit 3.2 (Verity Software House).

qRT-PCR

Total RNA was isolated from bladder urothelia using RNeasy Mini Kit (Qiagen) and 2 μg of it was used for cDNA synthesis using High Capacity cDNA Reverse Transcription Kit (Applied Biosystem). Real-time PCR was carried out with 7500 System (Applied Biosystems) under 95°C for 15′ for the first cycle; 95°C for 15″, 58°C for 20″ and 72°C for 30″ for 50 cycles, and 72°C for 5′ for the last cycle. PCR products were quantified by direct SYBR Green incorporation, with the relative abundance expressed as ratios to β-actin. The primers were: p19ARF-forward: gtcgcaggttcttggtcact, p19ARF-reverse: cgaatctgcaccgtagttga; p53-forward: agagaccgccgtacagaaga, p53-reverse: ctgtagcatgggcatccttt; p21-forward: cggtggaactttgacttcgt, p21-reverse: cagggcagaggaagtactgg.

Western blotting, histologic, IHC, and immunofluorescent staining

Total proteins from mouse urothelia or cultured RT4 cells were dissolved in a lysis buffer [10% SDS, 20 mmol/L Tris/HCl (pH7.5), 50 mmol/L NaCl, 5 mmol/L β-mercaptoethanol, and a mixture of protease inhibitors]. After SDS-PAGE, the proteins were transferred onto PVDF membrane and reacted consecutively with primary (Supplementary Table S1) and peroxidase-conjugated secondary antibodies.

Freshly dissected urinary bladders were fixed in PBS-buffered 10% formalin and embedded routinely in paraffin. Sections (4 μm) were stained with hematoxylin and eosin (H&E) for histologic examination. For IHC, deparaffinized sections were microwaved in a citrate buffer (pH 6.0) for 20 minutes to unmask the antigens and then incubated with primary (Supplementary Table S1) and secondary antibodies conjugated with horseradish peroxidase.

Statistical analysis

A Student *t* test (two tailed) was used to evaluate the statistical significance between *Upk2*-HRAS* mice and wild-type (*Upk2*-cre) mice in urothelial expression of p53 pathway components and between different groups of stably transfected cultured cells in their proliferation and invasion rates, with P value <0.05 considered statistically significant.

Results

Oncogenic HRAS*-induced persistent urothelial hyperplasia results from an equilibrium between mitogenic signals and antitumor defenses

A highly reproducible phenotype in transgenic mice bearing a single copy of oncogenic HRAS* under the control of the UPII promoter (*Upk2*-HRAS*) was the persistent urothelial hyperplasia (24). Compared with normal urothelium from the wild-type littermates (Fig. 1A, a), the hyperplastic lesions of the *Upk2*-HRAS* mice appeared as highly thickened, nonetheless well-differentiated urothelia with excellent polarity (Fig. 1A, b–d), and retention of superficial umbrella cells (arrows in Fig. 1A, c and d); and they started around 2 months of age and persisted through 12 months, without progressing, in grade or stage, to full-fledged urothelial tumor or reverting to normal urothelium. To understand the molecular underpinning of this phenomenon, we examined the cell-cycle status and found that at the steady state, there was a significant reduction of G_0–G_1 urothelial cells and increase of G_2 cells in *Upk2*-HRAS* transgenic mice (12 months of age), as compared with the wild-type controls (Fig. 1B, top). This corresponded well with elevated mitogenic signals including phosphorylated ERK and AKT (both T308 and S473) in the transgenic mice (Fig. 1B bottom and Supplementary Fig. S1). However, S-phase cells were not significantly higher (Fig. 1B), suggesting that the DNA synthesis was held in check and that a prolonged G_2 arrest existed, possibly due to concurrent induction of growth inhibitors/tumor suppressors (28). Of the tumor-suppressive pathways surveyed, that of p53, including p19, p53, and p21, exhibited marked upregulation on mRNA (Fig. 1C, left) and protein (Fig. 1C, right) levels. Such overt upregulation was not observed in pRB family proteins (e.g., pRB, p107, and p130). Interestingly, factors key to promoting G_2–M transition such as CDC2 and CYCLIN B1 were significantly downregulated in the hyperplastic lesions of the *Upk2*-HRAS* mice (Fig. 1D), a phenomenon observed in nonurothelial cells with an upregulated p53 pathway (28). Our results suggest that oncogenic HRAS*-triggered proliferative forces are counter

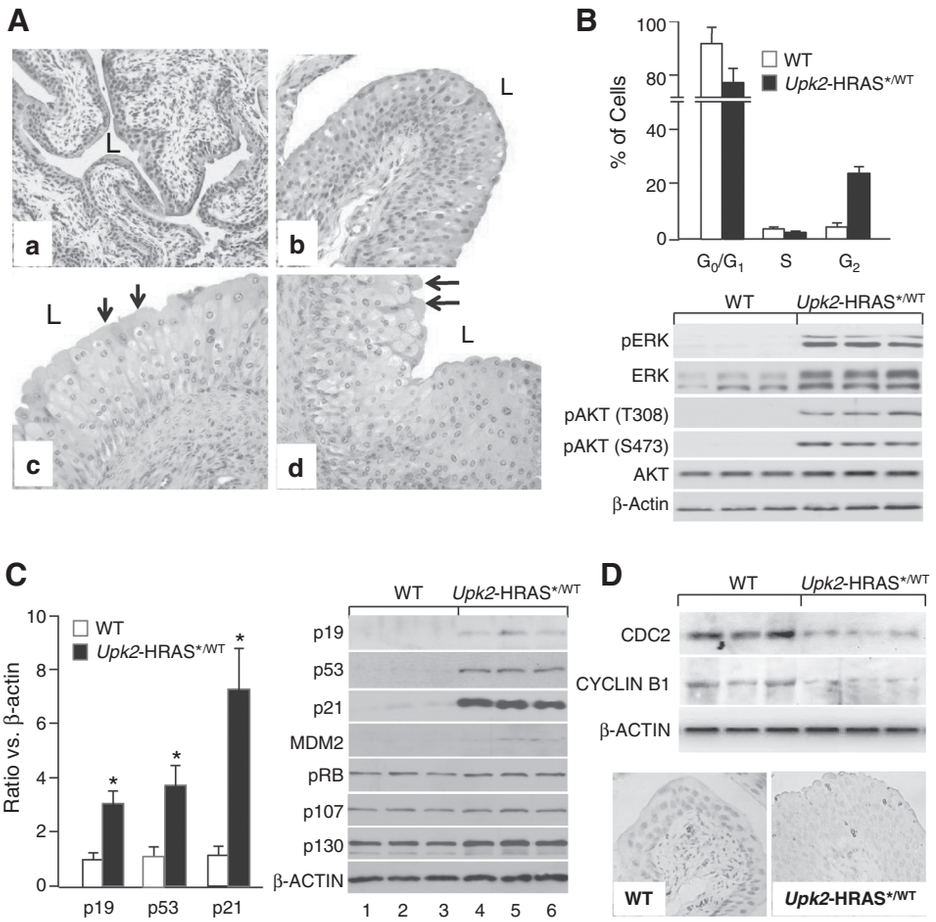

Figure 1.
Simultaneous induction of pro- and antimitogenic signals in transgenic mice expressing oncogenic HRAS* in urothelia, leading to persistent nonprogressive hyperplasia. Urothelia from *Upk2*-HRAS*$^{/WT}$ transgenic mice and wild-type littermates were subject to histopathology (A), flow cytometry (B, top), Western blotting of key RAS-downstream effectors (B, bottom), real-time PCR of p53 pathway components (C, left), Western blotting of key tumor suppressors (C, right), and Western blotting (D, top), and IHC staining of promoters of G_2–M transition CDC2 and CYCLIN B1 (D, bottom). Note that the WT mouse [12-month-old (A,a)] exhibited normal urothelium, whereas the *Upk2*-HRAS*$^{/WT}$ transgenic mice (A,b, A,c, and A,d, 4-, 8- and 12-months, respectively) exhibited urothelial hyperplasia. Note the reduced G_0–G_1 and increased G_2 phase (B, top) and elevated pERK and pAKT (B, bottom) in the transgenic mouse urothelia as compared with the WT controls. Note the significant overexpression (*, $P < 0.01$ compared to WT) of p19, p53, and p21 on both mRNA (C, left) and protein level (C, right) and largely unchanged pRB family proteins in the transgenic mice. Also note the reduced levels of CDC2 and CYCLIN B1 in the *Upk2*-HRAS*$^{/WT}$ transgenic mice (D). Magnification, ×200 in A and D.

balanced by antiproliferative forces, especially by the p53 signaling axis, thus reaching an equilibrium and resulting in a nonprogressive and nonregressive state of persistent urothelial hyperplasia, that is quite different from oncogenic RAS-induced premature senescence and apoptosis in primary-cultured cells (29).

Removal of p53 confers invasive property to cultured noninvasive urothelial tumor cells expressing oncogenic HRAS*

To determine whether the tumor-barrier effects of p53 upregulation by oncogenic HRAS* in urothelial cells were coincidental or causative, we introduced oncogenic HRAS* along with shRNA of p53 into cultured RT4 cells, which were originally derived from a human low-grade, superficial papillary bladder tumor (27) and lacked RAS or p53 mutation/deletion (30). Enforced expression of oncogenic HRAS* in RT4 elicited a marked upregulation of p53 and p21 (Fig. 2A). Knockdown of p53 or that along with the expression of a wild-type HRAS enhanced cell proliferation (Supplementary Fig. S2), but only slightly increased cell migration and invasion (Fig. 2C). In contrast, knocking down p53 and expressing an oncogenic HRAS* resulted in a dramatic increase of cell migration and invasion of RT4 cells (Fig. 2C and D). Thus, p53 deficiency and RAS activation appear to be synergistic in conferring the invasive property to human urothelial tumor cells and triggering the conversion of noninvasive human urothelial tumor cells into invasive ones.

Conditional compound mice expressing oncogenic HRAS* and lacking p53 develop high-grade, muscle-invasive urothelial carcinoma

To further define the interactive effects between oncogenic HRAS* and p53 deficiency *in vivo*, we developed compound mice by ablating p53 from urothelial cells expressing oncogenic HRAS*. To do so, we cross-bred three independent mouse lines: *Upk2*-HRAS* (24), *Upk2*-cre (in which the UPII drives the expression of a cre recombinase in urothelium; ref. 25), and floxed p53 (in which the exons of 5 and 6 were flanked by two loxP sites; Fig. 3A; ref. 26). We chose four resultant genotypes for phenotypic analyses: (i) *Upk2*-cre (as negative controls), (ii) *Upk2*-HRAS*$^{/WT}$, (iii) *Upk2*-cre/p53$^{LOX/LOX}$, and (iv) *Upk2*-HRAS*$^{/WT}$/*Upk2*-cre/p53$^{LOX/LOX}$ (Fig. 3B and C). These four groups were followed for 16 months and, upon histopathological examination, the *Upk2*-cre and Upk2-cre/p53$^{LOX/LOX}$ lines exhibited normal urothelia, and the *Upk2*-HRAS*$^{/WT}$ line exhibited urothelial hyperplasia, as expected, throughout the 16-month observation (Fig. 3D). In stark contrast, the compound line expressing oncogenic HRAS* and lacking p53 developed exclusively high-grade bladder tumors in the form of CIS and muscle-invasive tumors (Fig. 3C and D and Fig. 4A–

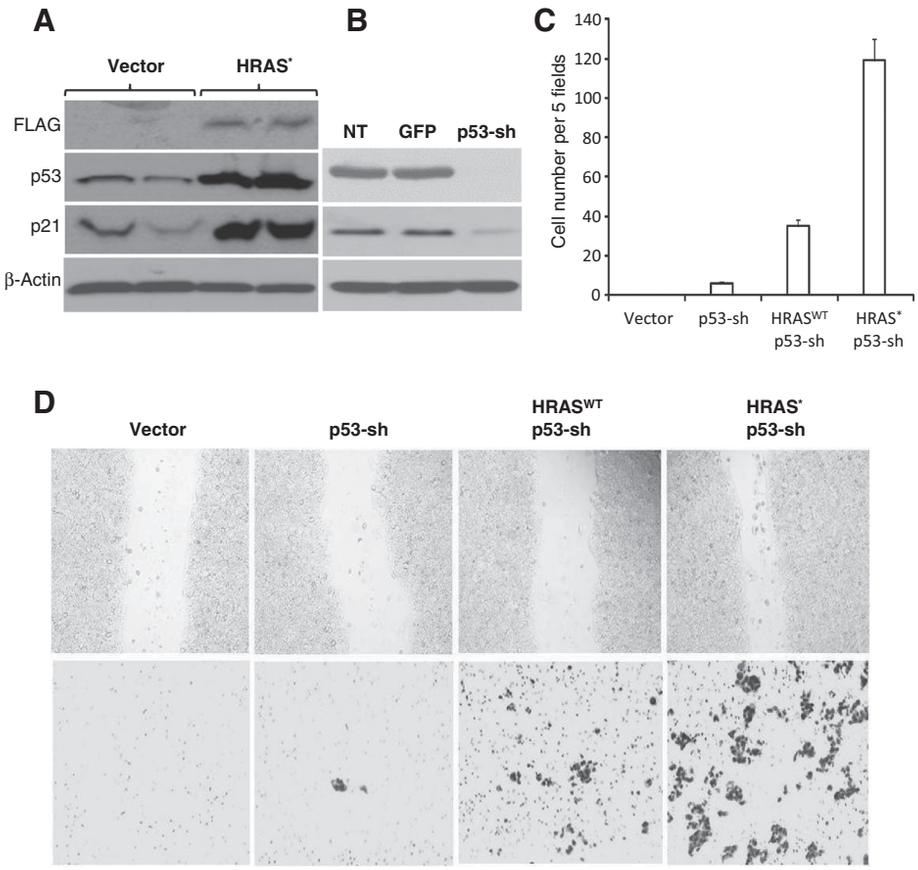

Figure 2.
Combined effects of oncogenic HRAS* and p53 deficiency on cultured urothelial cells. A, Western blotting showing that cultured RT4 cells stably transfected with FLAG-tagged HRAS* overexpressing p53 and p21, compared with vector-only transfected cells. B, Western blotting showing that RT4 cells stably transfected with shRNA of p53 had marked decrease of p53 itself and p21. RT4 cells stably transfected with shRNA of GFP served as a negative control. NT, no transfection. C, cell invasion assay using Matrigel [invasive cells counted per 5 high-powered (×200) fields microscopically] showing a very small increase of invasive cells in p53-knockdown cells, a moderate increase in p53-knockdown/WT-HRAS coexpressing cells, and a marked increase in p53-knockdown/HRAS* coexpressing cells. D, microscopic images of wound-healing (top) and Matrigel-invasion (bottom) experiments showing marked increase of both cell migration and invasion in cells coexpressing HRAS* and p53-shRNA.

C and E–G). The invasive tumors arose as early as 6 months of age and, by 16 months, a majority (60%) of the mice harbored muscle-invasive bladder tumors (Fig. 3C). The CIS lesions were relatively flat with microinvasive lesions in adjacent lamina propria (Fig. 4B and C). The microinvasive and muscle-invasive lesions were confirmed by cytokeratin 5 staining (Fig. 4D, H, and I). These lesions bear strong resemblance to those found in human patients with muscle-invasive urothelial carcinoma, and lend strong support to the sequence of urothelial tumor progression from CIS to invasive tumors (13, 14, 31, 32). Finally, focal squamous differentiation within the muscle-invasive lesions was common as evidenced by H&E staining and by IHC staining using antibodies against keratin 1 and TRIM29 (Supplementary Fig. S3), markers for identifying squamous components in human muscle-invasive urothelial carcinomas (33).

Epithelial-to-mesenchymal transition signifies CIS-invasive tumor conversion

That compound mice urothelially expressing oncogenic HRAS* and lacking p53 developed CIS and then invasive lesions also provided a unique opportunity for us to utilize these well-defined lesions to identify the molecular events that underlie this poorly defined progression step. Toward this end, we performed laser-capture microdissection of normal urothelia from the *Upk2*-cre mice, and CIS and muscle-invasive lesions from *Upk2*-HRAS$^{*/WT}$/*Upk2*-cre/p53$^{LOX/LOX}$ compound mice. After high-quality mRNAs were isolated from freshly dissected lesions, the cDNAs were hybridized to oligonucleotide arrays representing all mouse genes (Affymatrix). Of differentially upregulated genes, those functioning in the EMT dominate the muscle-invasive lesions when CIS lesions were used as a reference (Table 1). Three groups of genes were particularly worth noting: (i) transcription factors that drive EMT [e.g., twist homolog 1 (TWIST), zinc finger E-box binding homeobox 2 (ZEB2), and ZEB1]; (ii) matrix-degrading enzymes (e.g., matrix metallopeptidases 13, 3, 2 and 9); and (iii) extracellular matrix components [e.g., collagen (type I, III, and IV), versican, vimentin, and fibronectin; Table 1]. Not surprisingly, those upregulated in the muscle-invasive tumor/CIS comparison were also upregulated in the muscle-invasive tumor/normal urothelium comparison. However, few of those upregulated in muscle-invasive tumors were also upregulated in the CIS lesions, indicating that the EMT genes are primarily switched on during muscle invasion. The only genes that showed more than 2-fold increase in CIS over normal urothelium were matrix metalloproteinase (MMP)-13 and platelet-derived growth factor receptor, suggesting their potential role(s) in CIS formation. Antibody staining confirmed that MMP2, 3, 9, and 13 were all overexpressed almost exclusively in the muscle-invasive lesions, with MMPs 2 and 9 primarily associated with tumor cells and MMP3 and 13 in both tumor cells and matrix (Fig. 5).

EMT occurs in urothelial carcinoma progenitor/stem cells

To explore whether overexpression of EMT drivers occurred in more differentiated urothelial cells or in progenitor cells thus

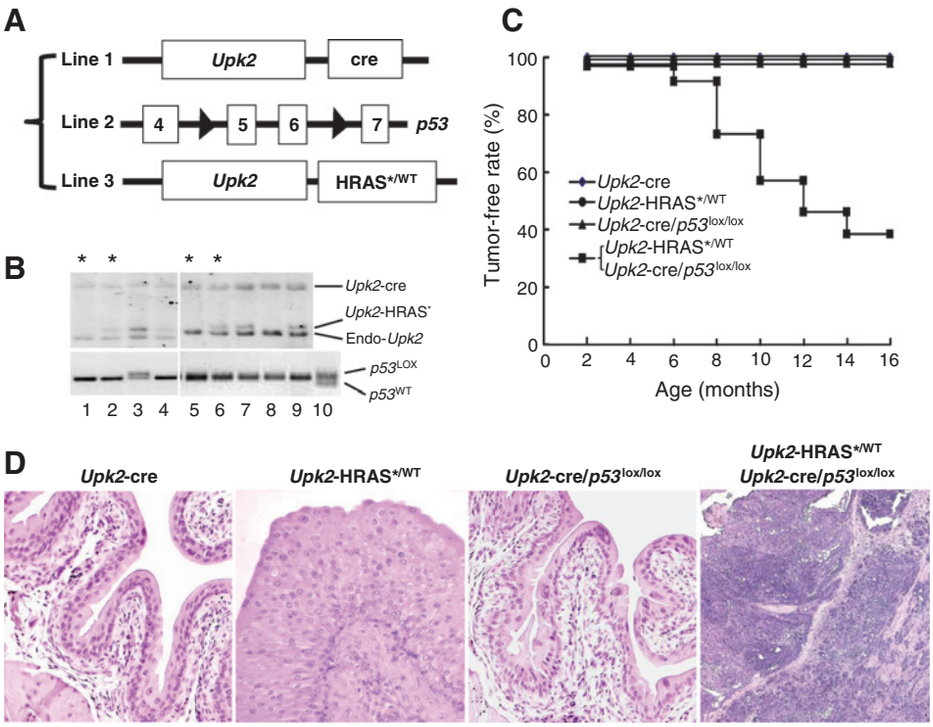

Figure 3.
Inactivation of p53 in urothelial cells of transgenic mice expressing oncogenic HRAS*. A, three transgenic lines for intercrossing contained transgene of uroplakin II promoter (*Upk2*) driving cre recombinase (Line 1); floxed p53 where exons 5 and 6 were flanked by loxP sites (Line 2); and *Upk2* driving oncogenic HRAS* (Line 3). B, offspring of two representative crosses were genotyped by Southern blotting of restriction-digested tail genomic DNA (top) using a mouse *Upk2* probe, revealing the 5.4-kB *Upk2*–cre transgene fragment, the 1.4-kB *Upk2*-HRAS* fragment, and the 1.1-kB endogenous *Upk2* fragment (endo-*Upk2*). The same DNA samples were subject to PCR using primers specifically detecting the first loxP site of the p53-mutant allele. Asterisks denote the four major genotypes chosen for additional analyses (also see C). C, the rate of the four major genotypes free of high-grade muscle-invasive urothelial carcinoma (tumor-free rate). Note that only mice expressing oncogenic HRAS* as well as lacking p53 in urothelia developed invasive urothelial carcinoma. D, representative H&E images of the four genotypes (all 8-month-old; see text). Magnification, ×200.

potentially playing a role in invasive tumor initiation, we performed IHC and double- and triple-immunofluorescent localization. Both ZEB1 and ZEB2 were strongly labeled in the nuclei of the invasive tumors cells of *Upk2*-HRAS$^{*/WT}$/*Upk2*-cre/p53$^{LOX/LOX}$ compound mice, but were barely detectable in normal urothelia of *Upk2*-cre or *Upk2*-cre/p53$^{LOX/LOX}$ mice and were only weakly labeled in *Upk2*-HRAS* mice (Fig. 6A and B). Upon triple fluorescent staining, ZEB2 was found to be associated with cells specifically expressing CD44, a urothelial/carcinoma progenitor cell marker (Fig. 6C; refs. 18, 19, 34). Interestingly, these ZEB2- and CD44-positive cells had a marked decrease of E-cadherin, an epithelial marker (35), and a marked increase of vimentin, a mesenchymal cell marker (Fig. 6C; ref. 36). Double staining of ZEB2 with keratin 14, another urothelial progenitor cell marker (34), again showed excellent colocalization (Fig. 6D). Whereas normal-appearing urothelial regions showed K14-positive cells that lacked ZEB2 labeling, areas with tumor morphology showed strong coexpression of ZEB2 and K14 (Fig. 6D). Furthermore, areas with leading edge of invasion showed strong ZEB2 and K14 coexpression (Fig. 6D). Interestingly, invasive tumors cells of the *Upk2*-HRAS$^{*/WT}$/*Upk2*-cre/p53$^{LOX/LOX}$ compound mice, but not the noninvasive cells of the single transgenic mice, strongly coexpressed in the nuclei activated AKT, activated β-catenin and ZEB2 (Supplementary Fig. S4), suggesting this signaling pathway as the underlying cause of EMT activation. These results establish that urothelial tumor progenitor cells in our compound transgenic mice expressing oncogenic HRAS* and lacking p53 strongly express EMT drivers and their expression may play a central role in initiating muscle-invasive urothelial carcinoma. Finally, in contrast with the expansion of K14-positive cells in the muscle-invasive lesions, cells positive for keratin 20, a marker expressed in urothelial superficial umbrella cells and used for terminal differentiation of normal urothelium (37), were completely absent from the muscle-invasive lesions (Supplementary Fig. S5). These results, together with our observation of focal squamous differentiation of the muscle-invasive lesions, strongly indicate that the muscle-invasive urothelial carcinoma of the bladder that we observed in our *Upk2*-HRAS*/*Upk2*-cre/p53$^{LOX/LOX}$ mice belongs to the "basal-subtype" recently classified in patients (4–6, 8–10).

Discussion

The recent expansion of whole-genome and whole-exome sequencing into a broad range of human cancers has yielded unprecedented details about somatic gene mutations, making it possible to classify cancers in genomic terms and to devise target-specific, precision therapies (38). Urothelial carcinoma of the bladder (UCB) is no exception. In a landmark paper (23), The

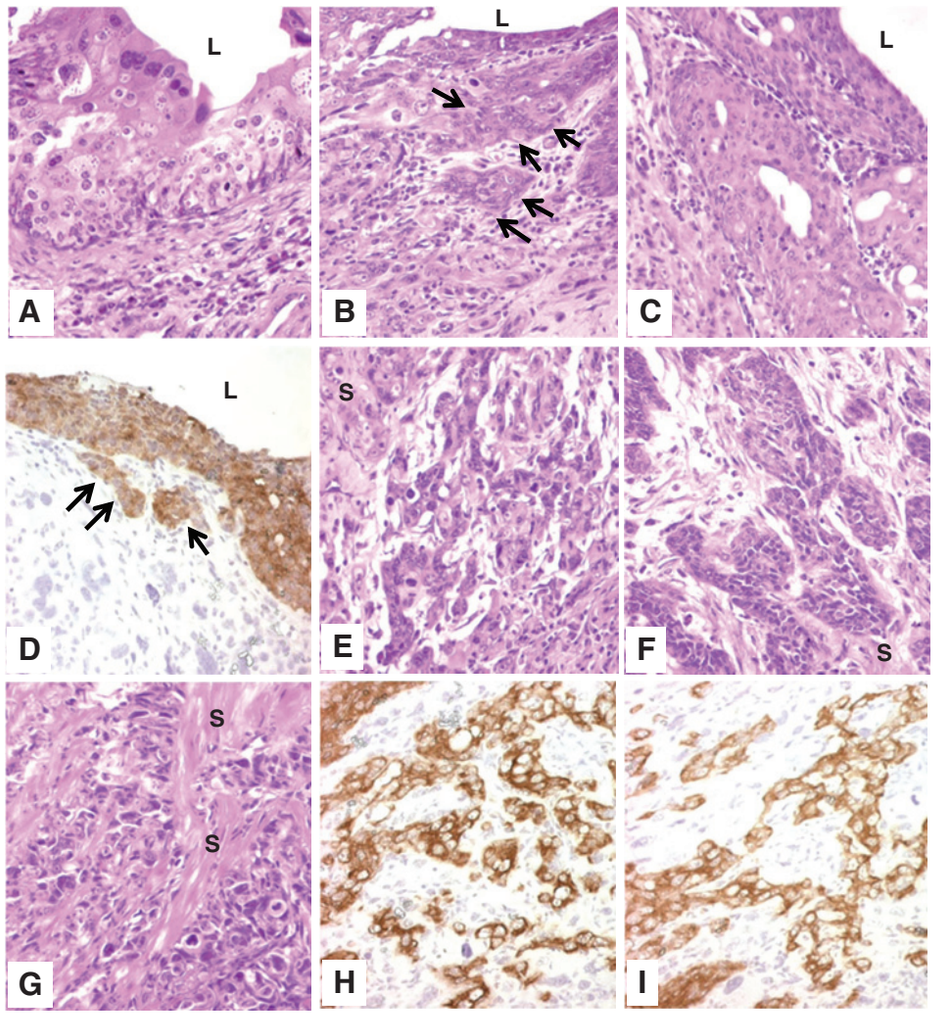

Figure 4.
Morphologic features of urothelial lesions in compound transgenic mice expressing oncogenic HRAS* and lacking p53. Urinary bladders of transgenic mice expressing oncogenic HRAS* and lacking p53 (8–12 month old) were stained by H&E (A–C; E–G) or anti-keratin 5 (D, H, and I). Note the high-grade lesions resembling carcinoma-in-situ (A–C) with lamina propria invasion (B and D, arrows) and muscle-invasive lesions (E–G) that were strongly labeled (brown) by anti-keratin 5 (D, H and I). L, lumen. S, smooth muscle. Magnification, ×200 for all panels.

Cancer Genome Atlas (TCGA) Research Network reported a comprehensive, multiplatform analysis of 131 high-grade, MIUCB on their somatic mutation, DNA copy number, messenger and miRNA expression, protein and phosphorylated protein expression, and DNA methylation. Of the several surprises from that report, one relates to the high frequency of alterations in the RTK/RAS/PIK3K signaling axis. Up to 72% of the high-grade MIUCB harbored activation mutations in the FGFR3, EGFR, ERBB2, ERBB3, HRAS/NRAS, and PIK3CA or inactivating mutations in NF1, PTEN, INPP4B, STK11, TSC1, and TSC2 (23). This is surprising because alterations in this pathway were previously assigned primarily to low-grade, noninvasive UCB and to predict low risk of progression and favorable clinical outcome (13, 21, 22), a concept supported by independent studies using genetically engineered mice. For instance, urothelial expression of an FGFR3 mutant (K644E) that constitutively activates the tyrosine kinase of FGFR3, either alone or in combination with KRAS and β-catenin mutations or with PTEN deletion, in transgenic mice failed to elicit any urothelial carcinoma (39). Similarly, urothelial overexpression of an EGFR in our transgenic mice induced proliferation but not tumor formation even after an exhaustively long (28-month) follow-up (40). Furthermore, urothelium-specific expression in our transgenic mice of oncogenic HRAS* at a level comparable with the endogenous RAS elicited urothelial hyperplasia that only occasionally progressed to low-grade, papillary noninvasive UCB in aged mice (>12 months; ref. 24). High-grade MIUCB was never observed in any of these RTK/RAS pathway-activated mouse models (24, 39, 40). The fact that gene mutations that activate the RTK/RAS pathway are highly prevalent in human high-grade MIUCB from the TCGA study (23) raises an important question as to whether these mutations are tumor "drivers" or "passengers" and whether the mutations require additional genetic alterations to be tumorigenic.

Our present study provides experimental evidence establishing that RAS activation per se is nontumorigenic in urothelial cells *in vivo* due, in large part, to a compensatory tumor barrier that RAS elicits in the p53 tumor suppressor pathway (Figs. 1 and 2 and Supplementary Fig. S1). Although p53 deficiency by itself is also nontumorigenic, it is highly synergistic with RAS activation, and these two alterations together are necessary and sufficient to initiate high-grade, CIS and MIUCB (Figs. 3 and 4). Of note, the MIUCB we observed in our double transgenic mice expressing oncogenic Ha-RAS and lacking p53 bears strong resemblance to the basal subtype of MIUCB recently classified in patients (4–11) in their (i) high expression of basal cell markers such as K5, K14, and CD44 (Figs. 4 and 6 and Supplementary Fig. S5); (ii) low or lack of expression of

Table 1. Differential expression of genes important for EMT between MIUCB, CIS, and normal urothelium

Gene name	CIS vs. normal urothelium	MIUCB vs. normal urothelium	MIUCB vs. CIS
Matrix metallopeptidase 3	−1.26	339.46	427.06
Matrix metallopeptidase 13	4.04	732.76	181.25
Collagen, type I, α 2	1.39	84.52	60.83
Secreted frizzled-related protein 2	−1.56	34.86	54.23
Versican	−1.63	24.55	39.99
Insulin-like growth factor binding protein 4	1.97	77.03	39.14
Collagen, type III, α 1	−1.89	19.24	36.32
Matrix metallopeptidase 2	1.09	38.11	34.92
Collagen, typeV, α 2	−1.05	29.23	30.65
Lysyl oxidase	−1.16	26.38	30.64
Secreted frizzled-related protein 1	−1.10	20.77	22.88
Fibroblast growth factor receptor 1	−4.50	3.24	14.59
Vimentin	1.46	20.30	13.91
Platelet derived growth factor receptor, β polypeptide	4.23	54.52	12.88
Transforming growth factor, β 2	−2.37	4.88	11.56
Twist homolog 1/Twist-Related Protein 1	−1.09	9.84	10.77
Zinc finger E-box binding homeobox 2	1.50	14.60	9.73
Fibronectin 1	1.32	11.13	8.44
Calcium/calmodulin-dependent protein kinase II inhibitor 1	1.56	12.23	7.84
Zinc finger E-box binding homeobox 1	1.35	9.38	6.97
Wingless-type MMTV integration site 9A	−1.57	4.21	6.60
Wingless-related MMTV integration site 7A	1.23	7.53	6.14
Transforming growth factor, β 3	1.20	6.87	5.73
Wingless-related MMTV integration site 2	−1.93	2.32	4.47
Matrix metallopeptidase 9	1.67	7.29	4.36
FGF13	−1.05	3.83	4.04
Wingless related MMTV integration site 10a	1.23	4.76	3.86
FGF7	−1.23	2.96	3.64
Transcription factor4	1.33	4.62	3.47
Thymoma viral proto-oncogene 3	1.89	5.80	3.07
Recombination signal binding protein for immunoglobulin kappa J region	1.14	3.35	2.93
Wingless-related MMTV integration site 5B	−1.53	1.64	2.51
PI3K, regulatory subunit 5	−1.16	2.17	2.51

NOTE: Laser-capture, microdissected tissues were subject to mRNA extraction/cDNA synthesis and expression array analysis (see Materials and Methods; GEO accession number: GSE64756). Fold changes in three pair-wise comparisons are shown, with ranking from the highest to the lowest (>2-fold) expression in consecutive order for the MIUCB/CIS comparison chosen for practical purposes (see text).

luminal cell markers such as E-cadherin and K20 (Fig. 6 and Supplementary Fig. S5); (iii) focal squamous differentiation (Supplementary Fig. S3); and (iv) high expression of EMT transcription factors (Twist, ZEB1, and ZEB2; Table 1; Fig. 6), EMT markers (vimentin, MMPs 2, 3, 9, and 13; Table 1; Figs. 5 and 6), and extracellular matrix components (collagen, versican, and fibronectin; Table 1). Our study therefore functionally defines RAS pathway activation and p53 deficiency as the highly synergistic codrivers for the basal-subtype MIUCB, and it has several significant implications. First, as has been demonstrated in other cancer types, tumor drivers (as opposed to the passengers) are more reliable biomarkers for cancer subclassification and prediction of chemotherapeutic response and clinical outcome (12). RAS pathway activation together with p53 deficiency could potentially serve as a new biomarker set for the genetic identification of the basal subtype of MIUCB that may be associated with an unfavorable prognosis, hence requiring aggressive therapeutic modalities. Second, our study reveals a previously unrecognized molecular cross-talk between RAS and p53 pathways in converting low-grade noninvasive urothelial lesions (e.g., hyperplasia and low-grade papillary) into becoming high-grade noninvasive (e.g., high-grade papillary and CIS) and invasive ones (e.g., MIUCB). Not only did we demonstrate such a relationship in transgenic mice (Figs. 3–6; Supplementary Figs. S3–S5), but we also showed that introducing oncongenic HRAS* and knocking down p53 in cultured RT4 cells confer invasive properties to these otherwise noninvasive human UCB cells (Fig. 2). It has been suggested, based on clinical longitudinal studies, that approximately 25% of the low-grade, noninvasive UCB can eventually progress in grade and/or stage to muscle invasion (41, 42). This occurs in an unpredictable manner that necessitates lifelong, vigilant follow-up by repeated cystoscopy and biopsy, a main cause for morbidity, time lost from work and high medical expenses. Thus far, no biomarker exists that can reliably predict the risk of progression of noninvasive UCB to the invasive stage (43, 44). Perhaps it is not surprising that p53 alterations are not very predictive of UCB progression (45), based on data from genetically engineered mice indicating the lack of tumorigenicity by p53 deficiency alone (Fig. 3; refs. 26, 46, 47). It is possible, however, that a combination of RAS pathway activation and p53 deficiency, as we demonstrated here, are better biomarkers for UCB surveillance and prediction of tumor progression. It is worth noting that ablation of both PTEN and p53 in mouse urothelia also led to MIUCB (48), consistent with the fact that PTEN acts in the RAS pathway and PTEN inactivation is functionally akin to RAS activation. Third, because RAS activation is a codriver of the basal-type MIUCB, inhibition of this pathway might be of significant value in treating and/or preventing the progression of this MIUCB subtype. The fact that the basal-type MIUCB in humans is often resistant to the existing chemotherapeutics (4) makes RAS pathway inhibition a particularly attractive avenue to explore. Because suppressing activated RAS per se remains challenging (49), it is likely that effectors of RAS will have to be targeted and that inhibition of more than one signaling branch (e.g., PI3K-AKT as well as MAPK) is required to

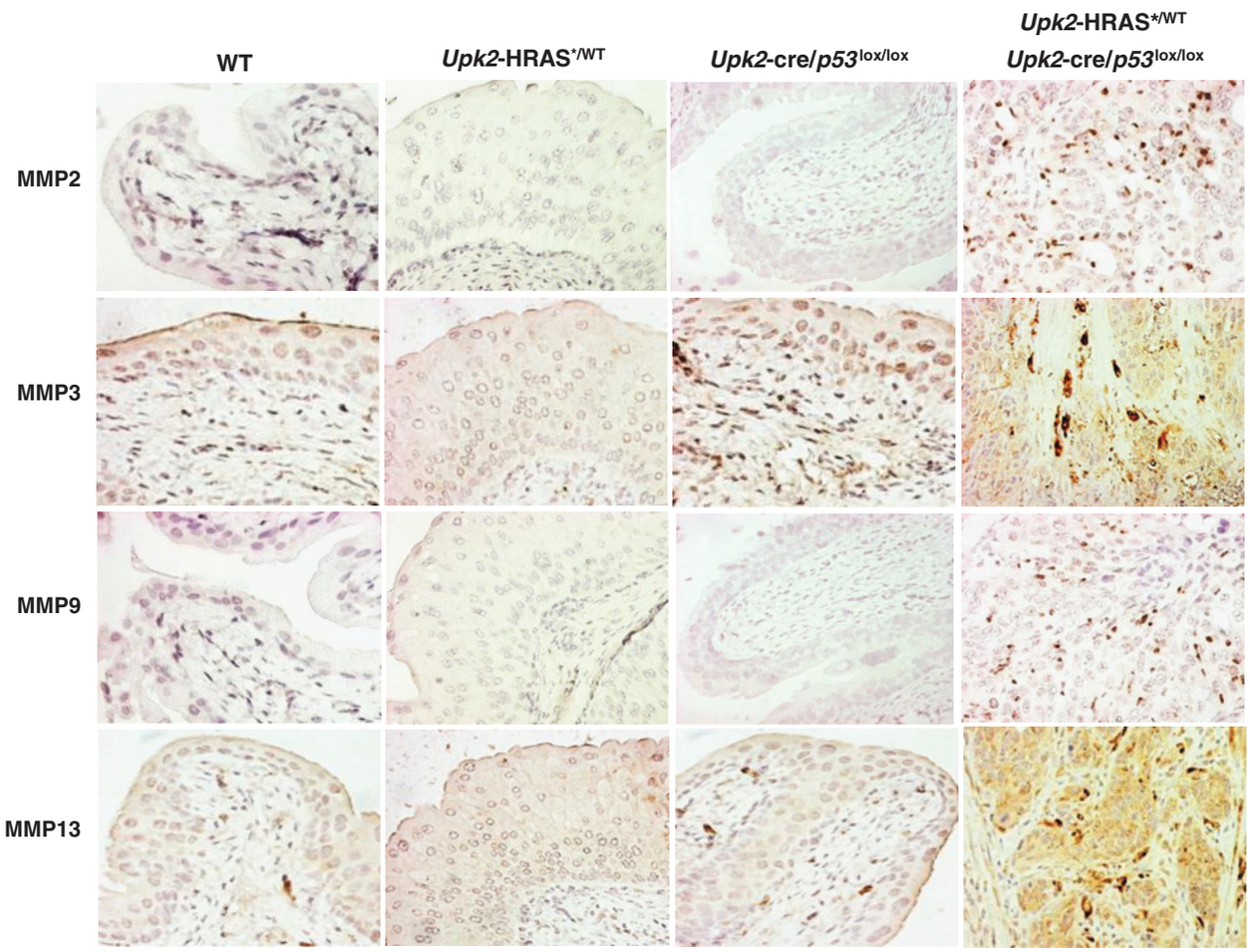

Figure 5.
Upregulation of MMPs in muscle-invasive urothelial carcinoma cells. Immunochemical staining using anti-MMP antibodies followed by hematoxylin counterstaining was performed on bladder tissues from age-matched (8-months) *Upk2*-cre, *Upk2*-HRAS*, *Upk2*-cre/p53$^{lox/lox}$, and *Upk2*-HRAS*/*Upk2*-cre/p53$^{lox/lox}$ mice. Note the significant upregulation of MMP2, MMP3, MMP9, and MMP13 in the muscle-invasive urothelial carcinoma cells of transgenic mice expressing the oncogenic HRAS* and deficient for p53. MMP3 and MMP13 were also detected strongly in some matrix cells. Magnification, ×200 for all panels.

achieve satisfactory results (50). Finally, the development of a new transgenic mouse model that consistently develops the basal-type MIUCB provides a novel *in vivo* platform for dissecting the evolutionary steps and the potential cross-talks among the different MIUCB subtypes and for testing subtype-specific diagnostic, preventive and therapeutic strategies. Clearly, many of these ideas require clinical validation studies before they can be translated to the bedside.

From a mechanistic standpoint, RAS activation and p53 deficiency could synergize on several fronts to affect cellular processes that govern urothelial tumorigenesis and progression. As shown recently, RAS activation increases the replicative pressure on urothelial cells, causing them to undergo DNA damage (51). Under normal circumstances, that is, when p53 pathway is intact, urothelial cells can sense DNA damage and upregulate p19Arf, which in turn upregulates p53 and downstream effectors such as p21 (Fig. 1). This helps restrain G_1–S and G_2–M transition and allow time for DNA damage repair to take place. When p53 pathway is defective, however, cell-cycle progression proceeds with amplification of the damaged DNA, setting a stage for malignant transformation. Another level of interaction is the collaborative nature of RAS activation and p53 deficiency on cell motility. Activated RAS is a strong enhancer of cell motility (52), whereas a functional p53 is a potent cell motility inhibitor (53). As we showed in our *in vitro* assay, activated RAS or p53 knockdown alone only had a marginal increase on cell motility, but combining these two events resulted in a marked increase of cell motility and triggered invasion (Fig. 2). Finally, as with other epithelial cells, RAS activation and p53 deficiency are both strong promoters of EMT (54, 55). The MAPK and AKT pathways, both shown to be prominently activated in our transgenic mice (Fig. 1 and Supplementary Fig. S1), can activate factors such as β-catenin that drive EMT (Table 1 and Supplementary Fig. S4). While normal p53 negatively regulates this process, p53 deficiency fuels EMT and sets the tumor cell invasion in motion (Figs. 2–6 and Supplementary Figs. S3–S5). There is mounting evidence suggesting that EMT can lead to drug resistance (35). Since EMT enhances the stemness and the plasticity of urothelial cells, it may also fuel the trans-differentiation of some of the urothelial progenitor cells toward the squamous lineage and squamous differentiation,

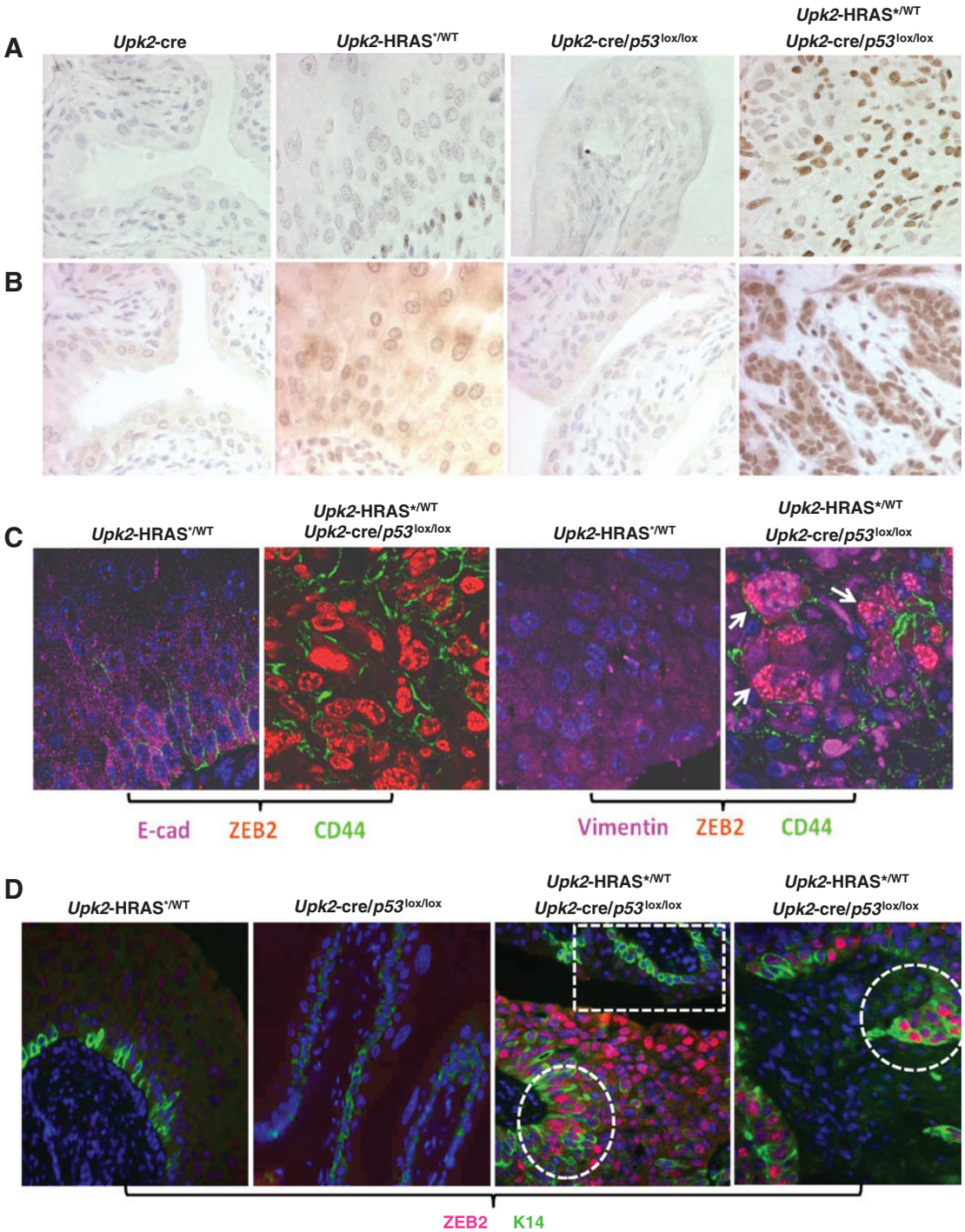

Figure 6.
Detection of transcriptional factors driving EMT in urothelial progenitor cells. A and B, urinary bladders from age-matched (8-months) *Upk2*-cre, *Upk2*-HRAS$^{*/WT}$, *Upk2*-cre/*p53*$^{lox/lox}$, and *Upk2*-HRAS$^{*/WT}$/*Upk2*-cre/*p53*$^{lox/lox}$ mice were immunohistochemically stained with anti-ZEB1 (A) and anti-ZEB2 (B) and counterstained by hemotoxylin. Note the marked upregulation of both proteins almost exclusively in the muscle-invasive lesions of the *Upk2*-HRAS$^{*/WT}$/*Upk2*-cre/*p53*$^{lox/lox}$ mice. C, urinary bladders from *Upk2*-HRAS$^{*/WT}$ and *Upk2*-HRAS$^{*/WT}$/*Upk2*-cre/*p53*$^{lox/lox}$ mice were triple stained using immuofluorescent method with anti-E-cadherin (E-cad), -ZEB2, and -CD44 (left two) or with anti-vimentin, -ZEB2, and -CD44 (right two). DAPI was used to visualize the nuclei. Note the marked downregulation of E-cadherin and dramatic upregulation of ZEB2 in CD44-positive cells in the muscle-invasive lesions of the *Upk2*-HRAS$^{*/WT}$/*Upk2*-cre/*p53*$^{lox/lox}$ mice. Also, note the colocalization of vimentin, ZEB2, and CD44 in the invasive tumor cells (far-right, arrows). D, urinary bladders from *Upk2*-HRAS$^{*/WT}$, *Upk2*-cre/*p53*$^{lox/lox}$, and *Upk2*-HRAS$^{*/WT}$/*Upk2*-cre/*p53*$^{lox/lox}$ mice were subject to immunofluorescent staining with anti-ZEB2 and -keratin 14 antibodies, with DAPI as counterstaining to visualize the nuclei. Note the lack of ZEB2 staining in K14-positive cells in *Upk2*-HRAS$^{*/WT}$ and *Upk2*-cre/*p53*$^{lox/lox}$ mice and the strong staining of ZEB2 in K14-positive cells in *Upk2*-HRAS$^{*/WT}$/*Upk2*-cre/*p53*$^{lox/lox}$ mice (middle, dashed circle). Dashed box illustrates an area of normal-appearing urothelium, showing the lack of ZEB2 staining. Also note that the leading edge of an early invasive lesion in *Upk2*-HRAS$^{*/WT}$/*Upk2*-cre/*p53*$^{lox/lox}$ mice had marked upregulation of ZEB2 in K14-positive cells (right). Magnification, ×200 for all panels.

another potential cause of drug resistance. In this regard, inhibiting RAS effectors that drive EMT and/or inhibiting EMT effectors such as MMPs may play a critical role in reducing chemoresistance that has been observed in the basal-type MIUCB (4). Because EMT is highly activated in progenitor/stem cells that give rise to the basal-type MIUCB (Fig. 6 and Supplementary Fig. S5), its suppression may present a unique opportunity for controlling the root cause of tumor cell expansion and invasion.

In summary, the data presented in this paper provide the first experimental evidence demonstrating that the loss of p53 is critical in allowing hyperplastic urothelial cells *in vivo* to bypass G_2 arrest induced by activated HRAS and proceed to tumor formation; that RAS pathway activation and p53 pathway inactivation together confer invasive properties to noninvasive urothelial tumor cells and these two synergistic events are necessary and sufficient to convert CIS to basal-subtype, MIUCB; and that activation of EMT and increased stemness in urothelial progenitor cells are crucial epigenetic events for invasive tumorigenesis. Our data also strongly suggest that increased urothelial plasticity due to EMT may underlie urothelial trans-differentiation to the squamous lineage, leading to focal squamous differentiation in urothelial carcinomas. From a clinical standpoint, combined RAS pathway activation and p53 pathway inactivation, events highly prevalent in human urothelial carcinomas as evidenced by whole-genome analyses, may serve as a new biomarker set to predict urothelial carcinoma progression, and inhibition of receptor tyrosine kinase/RAS pathway components may be used as therapeutic targets for basal-subtype, muscle-invasive urothelial carcinomas that are resistant to conventional chemotherapeutics.

Disclosure of Potential Conflicts of Interest

No potential conflicts of interest were disclosed.

Authors' Contributions

Conception and design: F. He, M.-S. Tang, C. Huang, X.-R. Wu
Development of methodology: F. He, X.-R. Wu
Acquisition of data (provided animals, acquired and managed patients, provided facilities, etc.): F. He, X.-R. Wu
Analysis and interpretation of data (e.g., statistical analysis, biostatistics, computational analysis): F. He, X.-R. Wu
Writing, review, and/or revision of the manuscript: F. He, J. Melamed, M.-S. Tang, C. Huang, X.-R. Wu
Administrative, technical, or material support (i.e., reporting or organizing data, constructing databases): F. He, J. Melamed
Study supervision: F. He, X.-R. Wu

Grant Support

This work was supported in part by grants from the United States NIH (P01 CA165980) and Veterans Affairs Office of Research and Development (Biomedical Laboratory Research and Development Service; 1I01BX002049) and a grant-in-aid from the Goldstein Fund for Urological Research of the New York University School of Medicine.

The costs of publication of this article were defrayed in part by the payment of page charges. This article must therefore be hereby marked *advertisement* in accordance with 18 U.S.C. Section 1734 solely to indicate this fact.

Received October 20, 2014; revised January 9, 2015; accepted February 3, 2015; published OnlineFirst March 20, 2015.

References

1. Lotan Y, Kamat AM, Porter MP, Robinson VL, Shore N, Jewett M, et al. Key concerns about the current state of bladder cancer: a position paper from the Bladder Cancer Think Tank, the Bladder Cancer Advocacy Network, and the Society of Urologic Oncology. Cancer 2009;115:4096–103.
2. Dancik GM, Theodorescu D. Pharmacogenomics in bladder cancer. Urol Oncol 2014;32:16–22.
3. Meeks JJ, Bellmunt J, Bochner BH, Clarke NW, Daneshmand S, Galsky MD, et al. A systematic review of neoadjuvant and adjuvant chemotherapy for muscle-invasive bladder cancer. Eur Urol 2012;62:523–33.
4. Choi W, Porten S, Kim S, Willis D, Plimack ER, Hoffman-Censits J, et al. Identification of distinct basal and luminal subtypes of muscle-invasive bladder cancer with different sensitivities to frontline chemotherapy. Cancer Cell 2014;25:152–65.
5. Damrauer JS, Hoadley KA, Chism DD, Fan C, Tiganelli CJ, Wobker SE, et al. Intrinsic subtypes of high-grade bladder cancer reflect the hallmarks of breast cancer biology. Proc Natl Acad Sci U S A 2014;111:3110–5.
6. Hurst CD, Knowles MA. Molecular subtyping of invasive bladder cancer: time to divide and rule? Cancer Cell 2014;25:135–6.
7. Riester M, Taylor JM, Feifer A, Koppie T, Rosenberg JE, Downey RJ, et al. Combination of a novel gene expression signature with a clinical nomogram improves the prediction of survival in high-risk bladder cancer. Clin Cancer Res 2012;18:1323–33.
8. Hoadley KA, Yau C, Wolf DM, Cherniack AD, Tamborero D, Ng S, et al. Multiplatform analysis of 12 cancer types reveals molecular classification within and across tissues of origin. Cell 2014;158:929–44.
9. Volkmer JP, Sahoo D, Chin RK, Ho PL, Tang C, Kurtova AV, et al. Three differentiation states risk-stratify bladder cancer into distinct subtypes. Proc Natl Acad Sci U S A 2012;109:2078–83.
10. Sjodahl G, Lovgren K, Lauss M, Patschan O, Gudjonsson S, Chebil G, et al. Toward a molecular pathologic classification of urothelial carcinoma. Am J Pathol 2013;183:681–91.
11. Huang HY, Shariat SF, Sun TT, Lepor H, Shapiro E, Hsieh JT, et al. Persistent uroplakin expression in advanced urothelial carcinomas: implications in urothelial tumor progression and clinical outcome. Hum Pathol 2007;38:1703–13.
12. Livshits G, Lowe SW. Accelerating cancer modeling with RNAi and non-germline genetically engineered mouse models. Cold Spring Harbor protocols 2013;2013.
13. Wu XR. Urothelial tumorigenesis: a tale of divergent pathways. Nat Rev Cancer 2005;5:713–25.
14. Dinney CP, McConkey DJ, Millikan RE, Wu X, Bar-Eli M, Adam L, et al. Focus on bladder cancer. Cancer Cell 2004;6:111–6.
15. Grossman HB. Superficial bladder cancer: decreasing the risk of recurrence. Oncology (Huntingt) 1996;10:1617–24.
16. Castillo-Martin M, Domingo-Domenech J, Karni-Schmidt O, Matos T, Cordon-Cardo C. Molecular pathways of urothelial development and bladder tumorigenesis. Urol Oncol 2010;28:401–8.
17. Wu XR, Kong XP, Pellicer A, Kreibich G, Sun TT. Uroplakins in urothelial biology, function, and disease. Kidney Int 2009;75:1153–65.
18. Gandhi D, Molotkov A, Batourina E, Schneider K, Dan H, Reiley M, et al. Retinoid signaling in progenitors controls specification and regeneration of the urothelium. Dev Cell 2013;26:469–82.
19. Van Batavia J, Yamany T, Molotkov A, Dan H, Mansukhani M, Batourina E, et al. Bladder cancers arise from distinct urothelial sub-populations. Nat Cell Biol 2014;16:982–91.
20. Shin K, Lim A, Odegaard JI, Honeycutt JD, Kawano S, Hsieh MH, et al. Cellular origin of bladder neoplasia and tissue dynamics of its progression to invasive carcinoma. Nat Cell Biol 2014;16:469–78.
21. Wolff EM, Liang G, Jones PA. Mechanisms of Disease: genetic and epigenetic alterations that drive bladder cancer. Nat Clin Pract Urol 2005;2:502–10.
22. van Rhijn BW, van der Kwast TH, Vis AN, Kirkels WJ, Boeve ER, Jobsis AC, et al. FGFR3 and P53 characterize alternative genetic pathways in the pathogenesis of urothelial cell carcinoma. Cancer Res 2004;64:1911–4.
23. Network TCGAR. Comprehensive molecular characterization of urothelial bladder carcinoma. Nature 2014;507:315–22.
24. Mo L, Zheng X, Huang HY, Shapiro E, Lepor H, Cordon-Cardo C, et al. Hyperactivation of Ha-ras oncogene, but not Ink4a/Arf deficiency, triggers bladder tumorigenesis. J Clin Invest 2007;117:314–25.

25. Mo L, Cheng J, Lee EY, Sun TT, Wu XR. Gene deletion in urothelium by specific expression of Cre recombinase. Am J Physiol Renal Physiol 2005; 289:F562–8.
26. He F, Mo L, Zheng XY, Hu C, Lepor H, Lee EY, et al. Deficiency of pRb family proteins and p53 in invasive urothelial tumorigenesis. Cancer Res 2009; 69:9413–21.
27. Rigby CC, Franks LM. A human tissue culture cell line from a transitional cell tumour of the urinary bladder: growth, chromosone pattern and ultrastructure. Br J Cancer 1970;24:746–54.
28. Taylor WR, Stark GR. Regulation of the G2/M transition by p53. Oncogene 2001;20:1803–15.
29. Lin AW, Barradas M, Stone JC, van Aelst L, Serrano M, Lowe SW. Premature senescence involving p53 and p16 is activated in response to constitutive MEK/MAPK mitogenic signaling. Genes Dev 1998;12:3008–19.
30. DeGraff DJ, Robinson VL, Shah JB, Brandt WD, Sonpavde G, Kang Y, et al. Current preclinical models for the advancement of translational bladder cancer research. Mol Cancer Ther 2013;12:121–30.
31. Cohen SM, Ohnishi T, Clark NM, He J, Arnold LL. Investigations of rodent urinary bladder carcinogens: collection, processing, and evaluation of urine and bladders. Toxicol Pathol 2007;35:337–47.
32. Dalbagni G, Presti J, Reuter V, Fair WR, Cordon-Cardo C. Genetic alterations in bladder cancer. Lancet 1993;342:469–71.
33. Huang W, Williamson SR, Rao Q, Lopez-Beltran A, Montironi R, Eble JN, et al. Novel markers of squamous differentiation in the urinary bladder. Hum Pathol 2013;44:1989–97.
34. Chan KS, Espinosa I, Chao M, Wong D, Ailles L, Diehn M, et al. Identification, molecular characterization, clinical prognosis, and therapeutic targeting of human bladder tumor-initiating cells. Proc Natl Acad Sci U S A 2009;106:14016–21.
35. McConkey DJ, Choi W, Marquis L, Martin F, Williams MB, Shah J, et al. Role of epithelial-to-mesenchymal transition (EMT) in drug sensitivity and metastasis in bladder cancer. Cancer Metastasis Rev 2009;28:335–44.
36. Kokkinos MI, Wafai R, Wong MK, Newgreen DF, Thompson EW, Waltham M. Vimentin and epithelial-mesenchymal transition in human breast cancer–observations *in vitro* and *in vivo*. Cells Tissues Organs 2007;185: 191–203.
37. Lopez-Beltran A, Montironi R, Vidal A, Scarpelli M, Cheng L. Urothelial dysplasia of the bladder: diagnostic features and clinical significance. Anal Quant Cytopathol Histopathol 2013;35:121–9.
38. Kandoth C, McLellan MD, Vandin F, Ye K, Niu B, Lu C, et al. Mutational landscape and significance across 12 major cancer types. Nature 2013; 502:333–9.
39. Ahmad I, Singh LB, Foth M, Morris CA, Taketo MM, Wu XR, et al. K-Ras and beta-catenin mutations cooperate with Fgfr3 mutations in mice to promote tumorigenesis in the skin and lung, but not in the bladder. Dis Model Mech 2011;4:548–55.
40. Cheng J, Huang H, Zhang ZT, Shapiro E, Pellicer A, Sun TT, et al. Overexpression of epidermal growth factor receptor in urothelium elicits urothelial hyperplasia and promotes bladder tumor growth. Cancer Res 2002;62:4157–63.
41. Knowles MA. Molecular subtypes of bladder cancer: Jekyll and Hyde or chalk and cheese? Carcinogenesis 2006;27:361–73.
42. Tanaka M, Grossman HB. Tumor suppressor genes of bladder cancer and potential for gene therapy. Adv Exp Med Biol 2003;539(Pt A):185–91.
43. Xylinas E, Kluth LA, Lotan Y, Daneshmand S, Rieken M, Karakiewicz PI, et al. Blood- and tissue-based biomarkers for prediction of outcomes in urothelial carcinoma of the bladder. Urol Oncol 2014;32:230–42.
44. Shirodkar SP, Lokeshwar VB. Potential new urinary markers in the early detection of bladder cancer. Curr Opin Urol 2009;19:488–93.
45. Stadler WM, Lerner SP, Groshen S, Stein JP, Shi SR, Raghavan D, et al. Phase III study of molecularly targeted adjuvant therapy in locally advanced urothelial cancer of the bladder based on p53 status. J Clin Oncol 2011; 29:3443–9.
46. Cheng J, Huang H, Pak J, Shapiro E, Sun TT, Cordon-Cardo C, et al. Allelic loss of p53 gene is associated with genesis and maintenance, but not invasion, of mouse carcinoma in situ of the bladder. Cancer Res 2003;63: 179–85.
47. Gao J, Huang HY, Pak J, Cheng J, Zhang ZT, Shapiro E, et al. p53 deficiency provokes urothelial proliferation and synergizes with activated Ha-ras in promoting urothelial tumorigenesis. Oncogene 2004;23:687–96.
48. Puzio-Kuter AM, Castillo-Martin M, Kinkade CW, Wang X, Shen TH, Matos T, et al. Inactivation of p53 and Pten promotes invasive bladder cancer. Genes Dev 2009;23:675–80.
49. Stephen AG, Esposito D, Bagni RK, McCormick F. Dragging ras back in the ring. Cancer Cell 2014;25:272–81.
50. Zhou H, Huang HY, Shapiro E, Lepor H, Huang WC, Mohammadi M, et al. Urothelial tumor initiation requires deregulation of multiple signaling pathways: implications in target-based therapies. Carcinogenesis 2012; 33:770–80.
51. Evangelou K, Bartkova J, Kotsinas A, Pateras IS, Liontos M, Velimezi G, et al. The DNA damage checkpoint precedes activation of ARF in response to escalating oncogenic stress during tumorigenesis. Cell Death Differ 2013; 20:1485–97.
52. Baker NM, Yee Chow H, Chernoff J, Der CJ. Molecular pathways: targeting RAC-p21-activated serine-threonine kinase signaling in RAS-driven cancers. Clin Cancer Res 2014;20:4740–6.
53. Muller PA, Vousden KH, Norman JC. p53 and its mutants in tumor cell migration and invasion. J Cell Biol 2011;192:209–18.
54. Turley EA, Veiseh M, Radisky DC, Bissell MJ. Mechanisms of disease: epithelial-mesenchymal transition–does cellular plasticity fuel neoplastic progression? Nat Clin Pract Oncol 2008;5:280–90.
55. Ansieau S, Courtois-Cox S, Morel AP, Puisieux A. Failsafe program escape and EMT: a deleterious partnership. Semin Cancer Biol 2011;21:392–6.